

SURFACE ENTHALPY OF GOETHITE

LENA MAZEINA AND ALEXANDRA NAVROTSKY*

Thermochemistry Facility and NEAT ORU, University of California at Davis, Davis, CA 95616, USA

Abstract—High-temperature oxide-melt solution calorimetry and acid-solution calorimetry were used to determine the heat of dissolution of synthetic goethite with particle sizes in the range 2–75 nm and measured surface areas of 30–273 m²/g ($27\text{--}240 \times 10^3 \text{ m}^2/\text{mol}$). Sample characterization was performed using X-ray diffraction, Fourier transform infrared spectroscopy, the Brunauer, Emmett and Teller method and thermogravimetric analysis. Water content (structural plus excess water) was determined from weight loss after firing at 1100°C. Calorimetric data were corrected for excess water assuming this loosely adsorbed water has the same energetics as bulk liquid water. The enthalpy of formation was calculated from calorimetric data using enthalpies of formation of hematite and liquid water as reference phases for high-temperature oxide-melt calorimetry and using enthalpy of formation of lepidocrocite for acid-solution calorimetry. The enthalpy of formation of goethite can vary by 15–20 kJ/mol as a function of surface area. The plot of calorimetric data vs. surface area gives a surface enthalpy of $0.60 \pm 0.10 \text{ J/m}^2$ and enthalpy of formation of goethite (with nominal composition FeOOH and surface area = 0) of $-561.5 \pm 1.5 \text{ kJ/mol}$. This surface enthalpy of goethite, which is lower than values reported previously, clarifies previous inconsistencies between goethite-hematite equilibrium thermodynamics and observations in natural systems.

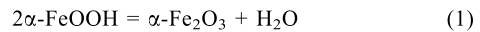
Key Words—Enthalpy of Formation, Goethite, Surface Enthalpy.

INTRODUCTION

Natural goethite (α -FeOOH) appears abundantly as a fine-grained material with a large surface area, allowing many processes in soil and sediments involving goethite to occur rapidly in the environment (Dixon, 1991; Cohen *et al.*, 1998). The surface functional groups (hydroxyl groups) are reactive with cations, anions, toxic and radioactive elements, living organisms, and organic materials in different sorption reactions (von Gunten *et al.*, 1999; Lower *et al.*, 2000; Lehmann *et al.*, 2001; Duff *et al.*, 2002; Kaiser, 2003; Kosmulski and Maczka, 2004). It is used as a catalyst in environmental applications (Ottley *et al.*, 1997; Li *et al.* 2003). Synthetic goethite is very often used as a model system in adsorption studies for various naturally occurring processes (Manceau and Charlet, 1994; Hiemstra and Van Riemsdijk, 1996; Crespo *et al.*, 2003; Kosmulski *et al.*, 2003). Therefore, the quantitative description of surface processes on goethite has widespread applications.

The distribution of functional groups as reactive sites depends on the available surface area of the sample. Free surface area not only influences the reactivity of the oxyhydroxide, it also influences phase transformation and thermodynamic stability (Cornell and Schwertmann, 1996; Navrotsky, 2004). Further, for a comprehensive analysis of all these processes, an understanding of the energetics associated with increasing the surface area is required.

Goethite has been investigated with respect to surface thermodynamics. Ferrier (1966) performed the most extensive investigation and reported the enthalpy of dissolution for variable sized samples of hematite and goethite, discussing the energetics of the goethite-hematite equilibrium according to reaction 1:



A major advantage of this work is that the calorimetric data were corrected for the presence of excess water. Additionally, the surface area was measured by the Brunauer, Emmett and Teller (BET) method which is generally both precise and accurate. However, there is inconsistency in the various reported data. Diakonov *et al.* (1994) performed a literature review, which also included Ferrier's data, to optimize the goethite surface thermodynamic properties. As data on surface area were lacking in many studies reviewed, Diakonov *et al.* (1994) had to approximate them from knowledge of the synthesis conditions. Moreover, they did not discuss the influence of excess water on the heat of goethite dissolution. Their estimated surface enthalpy was $1.55 \pm 0.20 \text{ J/m}^2$ which is slightly higher than the 1.25 J/m^2 reported by Ferrier (1966). This difference comes from the selection of data sets in Diakonov's study, the uncertainty in surface-area determination, and in the consideration of the influence of excess water on heat of dissolution. Based on this surface enthalpy data and estimated data for surface entropy, Diakonov *et al.* (1994) reported the surface free energy, ΔG_s^0 , at 25°C to be $1.4 \pm 0.2 \text{ J/m}^2$. Langmuir (1971) reported the surface free energy as 1.6 J/m^2 , which ignores surface entropy. Nevertheless, these publications did not report on the

* E-mail address of corresponding author:
anavrotsky@ucdavis.edu
DOI: 10.1346/CCMN.2005.0530201

enthalpy of desorption of adsorbed water. Initial attempts to consider this factor were made by Majzlan (2002).

Surface enthalpy for hematite obtained by Ferrier (1967) is 0.77 J/m² and surface free energy reported by Langmuir (1971) is 1.2 J/m². Despite the seemingly smaller surface energy of hematite than of goethite, the particle size of goethite coexisting with hematite is smaller than that of hematite. Also, the transformation of goethite to hematite under ambient conditions has not been observed (Langmuir, 1971). Moreover, one can see the opposite trend for the boehmite-corundum equilibrium (larger surface area for anhydrous phase) (Majzlan *et al.*, 2000). Consequently, the inconsistency of hematite and goethite relative energetics with *in situ* observations appears to require further investigation.

Our work addresses the effect of surface area on the thermodynamic stability of goethite, independent of the goethite-hematite equilibrium. We report new measurements of goethite surface enthalpy. We examine the presence of adsorbed surface water and dependence of enthalpy of the reaction goethite → hematite + water on particle size of goethite. The energetics of very fine-grained goethite particles with measured surface area as high as 273 m²/g (particle size ~2 nm) is studied for the first time. We obtained the formation enthalpy of goethite samples with particle sizes of 2–75 nm by high-temperature drop-solution calorimetry and acid-solution calorimetry. An advantage of high-temperature oxide-melt calorimetry is that goethite undergoes complete dehydration, dissolving as Fe₂O₃ with evolved gaseous H₂O, resulting in the same final states for all samples, independent of initial particle size. An advantage of acid-solution calorimetry is that it eliminates any possible concerns for significant dehydration upon dropping before entering the thermopile of the high-temperature calorimeter for hydrated goethite samples. However, coarse-grained goethite samples dissolve much more readily in an oxide melt than in aqueous acid. Thus, a wider sample-size range can be measured by high-temperature oxide melt calorimetry. Hence, the two methods are complementary and consistent results from both suggest that the measurements are free of problems.

Surface area was measured by gas adsorption (BET method, Brunauer *et al.*, 1938). This approach resolves uncertainties in estimates of surface area met in other general studies for fine-grained goethite. Direct measurements of both heat of dissolution and surface area of one mole of goethite avoid any ambiguities. This illuminates direct dependence of enthalpies on surface area.

In this paper, we report the experimental results and discuss values of enthalpy of formation and surface enthalpy obtained for goethite. Discussion on the application of high-temperature oxide-melt calorimetry in comparison to acid-solution calorimetry follows.

Comparison of goethite energetics with the energetics of other hydroxides and geological implications of the results conclude the article.

EXPERIMENTAL METHODS

Synthesis

Coarse-grained goethite (bulk) was synthesized by precipitation of 0.1 M Fe(NO₃)₃·9H₂O by 5 M KOH with vigorous stirring (Schwertmann and Cornell, 2000). The precipitate was diluted with water and aged for 70 h at 60°C.

Goethite 30 nm in size was prepared by hydrolysis of 1 M FeCl₃ solution at 80°C and adding 1 M NaOH (OH/Fe = 0.75). After the solution had been kept at room temperature for 50 h, 20 mL of 10 M NaOH solution were added. The suspension was then heated at 80°C in a closed polyethylene flask for 8 days. Since akaganeite often forms competitively with goethite (Schwertmann and Cornell, 2000), the temperature should be >70°C and hydrolysis should last several days to remove chloride completely, otherwise akaganeite will be formed.

Goethite 9 nm in size was synthesized by ageing a mixture of 2 M Fe(NO₃)₃·9H₂O solution (35 mL), of 1 M NaOH (140 mL) and 140 mL of water at room temperature for 50 days (Schwertmann and Cornell, 2000).

Goethite 7 nm in size was prepared by mixing a 0.5 M solution of Fe(NO₃)₃·9H₂O (60 mL) with 2.5 M KOH (250 mL) added at a rate of 10 mL/min with stirring (Lützenkirchen *et al.*, 2001). The mixture was then aged for 100 h at 60°C.

Fine-grained goethite (5 nm and 2 nm in size) was prepared using ammonium carbonate as the precipitation agent. 50 mL of 0.506 M FeCl₃ solution were added dropwise from a burette to a beaker containing ~1.5 L of ammonium carbonate solution (0.23 g/L). The pH value was maintained at 8 by adding (from a second burette) 5 M NaOH (for the 5 nm sample) and 1 M NH₄OH (for the 2 nm sample).

After precipitation, the solids were decanted, dialyzed for 2 weeks using VISKING dialysis tubing, type 36/32, changing water twice a day and then freeze dried. Hematite used as a reference material was prepared by heating the 5 nm goethite at 900°C for 12 h. All chemicals used were reagent grade from Alfa Aesar.

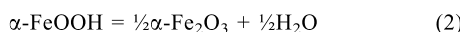
Characterization

After freeze drying, the samples were analyzed without further treatment. The X-ray diffraction (XRD) patterns were obtained using a Scintag PAD V diffractometer operating at 45 kV and 40 mA using CuK α (λ = 0.154056 nm) radiation. The diffractometer was calibrated using quartz as a standard. Patterns were collected from 10 to 70°2θ with a step size of 0.02°2θ and a dwell time of 15 s for fine-grained samples and 2 s for coarse-grained samples (bulk and 30 nm in size). The counting

time was chosen to obtain several thousand counts on the most intense diffraction maximum. Lattice parameters and the size of diffraction domain (particle size) of the samples were determined by Rietveld refinement using JADE 6.1 (Materials Data Inc., Livermore, 2001) and Material Studio (Accelrys Inc, 2004) software.

Fourier transform infrared (FTIR) spectra were collected with a Bruker Equinox 55 spectrometer using the KBr pellet technique. Pellets (13 mm diameter, 150 mg) were pressed until the mixture of KBr and sample became clear and the spectra were recorded immediately after pellet preparation. The spectrometer was flushed continuously with nitrogen to avoid contamination by atmospheric water and CO₂ during analysis. Spectra were collected in the 400–4000 cm⁻¹ range with a resolution of 4 cm⁻¹. A baseline correction was applied before interpretation.

Water content was determined in furnace experiments by heating the samples at 1100°C for 12 h. The amount of water adsorbed was calculated from weight loss over the stoichiometric weight loss (10.14 wt.%) for the reaction



Thermogravimetric analysis/differential scanning calorimetry (TGA/DSC) analyses were performed using a Netzsch 409 instrument for 30 nm and 5 nm samples in Ar atmosphere from 20 to 400°C at a heating rate of 20°C/min.

Surface area was measured by the BET method on a Micromeritics ASAP 2020 apparatus with preliminary sample degas in vacuum at 90°C for at least 10 h.

Scanning electron microscopy (SEM) (on an FEI XL30-SFEG instrument) and high-resolution transmission electron microscopy (HRTEM) (on an Topcon 002b instrument, LaB6 filament at 200 kV) images were

recorded to determine the morphology and crystal size. Carbon black standard Ted Pella #645 was used for TEM calibration.

Calorimetric measurements

For determination of enthalpies of formation of nano- and bulk goethite samples, a custom-built Tial-Calvet high-temperature microcalorimeter (Navrotsky, 1997) was used. Calibration used the heat content of ~5 mg of $\alpha\text{-Al}_2\text{O}_3$ pellets (99.997% metal basis, Alfa Aesar). The samples, in the form of ~5 mg pellets, were dropped into a Pt crucible containing a melt of composition 3Na₂O·4MoO₃ at 701°C which acts as solvent. The measured heat of drop solution (ΔH_{ds}) is the sum of heat content of the sample, enthalpy of solution and heat of H₂O evolution. The reaction tube in the calorimeter was flushed by oxygen (30 mL/min) to remove evolved water (Navrotsky *et al.*, 1994) and to maintain an oxidizing atmosphere. For fine-grained samples (2, 5, 7 and 9 nm) having hydration levels up to 0.818 moles of excess H₂O per mole of FeOOH, the enthalpy of solution was also measured in a Hart Scientific IMC-4400 isothermal calorimeter. Experiments were performed at 25°C using HCl (5.00 N standardized solution, Alfa Aesar). Calorimeter calibration was performed by dissolving KCl (NIST standard reference material 1655) in deionized water. The average weight of samples was ~5 mg. Coarser samples dissolved too slowly for accurate measurement.

RESULTS

X-ray powder diffraction analysis showed that all samples have the goethite orthorhombic structure with no additional phases (Figure 1). Crystallite size and lattice parameters are shown in Table 1.

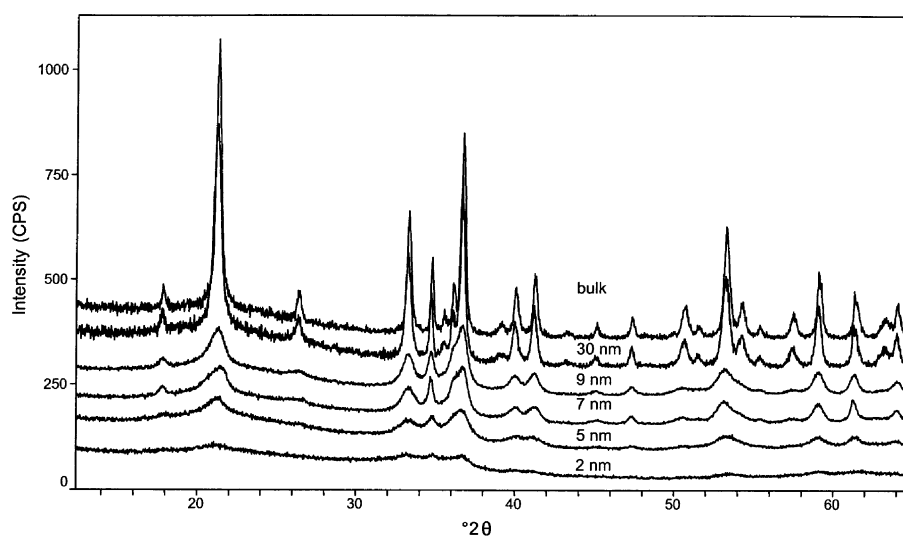


Figure 1. XRD pattern of nanophase goethites.

Table 1. Crystallite and particle size, surface area and water content as moles of excess water per mole of formula unit ($\text{FeOOH}\cdot x\text{H}_2\text{O}$) and lattice parameters for nanophasic oxides.

Crystallite size (nm) (XRD)	Weight loss upon firing (%)	x (mol)	Particle size (nm) (SEM/TEM)	Surface area (m^2/g) (BET)	Lattice parameters [§]		
					a (Å)	b (Å)	c (Å)
Bulk	11.5* \pm 0.1 [†] (5) [‡]	0.076 \pm 0.007 (5)	Rods 80 \times 2500	30.07 \pm 0.08	9.953(7)	3.021(5)	4.610(0)
30 nm	12.72 \pm 0.05 (6)	0.146 \pm 0.003 (6)	Rods 30 \times 400	52.6 \pm 0.2	9.951(5)	3.022(3)	4.608(6)
9 nm	17.3 \pm 0.1 (6)	0.40 \pm 0.02 (6)	Rods 10 \times 90	124.7 \pm 1.4	9.96(7)	3.03(3)	4.63(0)
7 nm	16.9 \pm 0.3 (6)	0.423 \pm 0.002 (6)	—	127.4 \pm 1.6	9.95(8)	3.025(7)	4.62(1)
5 nm	22.8 \pm 0.4 (6)	0.80 \pm 0.03 (6)	Rods 4 \times 40	238.1 \pm 2.6	9.95(5)	3.020(1)	4.61(4)
2 nm	23.08 \pm 0.09 (4)	0.818 \pm 0.006 (4)	—	273.4 \pm 2.5	9.95(9)	3.00(8)	4.59(8)
Hematite			Bulk	7.2 \pm 0.2		5.031	13.731

*average

[†] two standard deviations of the mean

[‡] number of measurements

[§] the digit in parentheses reflects the last valid digit

Analysis by FTIR revealed that all samples were pure α -FeOOH, except where one of the initial components was Fe nitrate (bulk, 7 nm and 9 nm samples). The presence of nitrate in these samples was attributed to adsorbed species as nitrate remains even after two weeks of dialysis and washing procedures. The amount of nitrate was analyzed commercially (Galbraith laboratories) and is <0.3 wt.%; therefore we can ignore its effect on the thermochemical data in those samples.

The results of the loss-on-ignition experiments and the water content as moles of excess water per mole of FeOOH are shown in Table 1. Weight-loss experiments showed increased excess water as particle size decreased. A strong correlation of the surface area and amount of excess water, x (Figure 2), suggests that most or all excess water is adsorbed on the surface. The TGA data agree with data obtained from furnace weight-loss experiments. The excess water (corresponding to the formula $\text{FeOOH}\cdot x\text{H}_2\text{O}$) is evolved completely at 100–130°C, suggesting that this H_2O is physisorbed and not strongly bound (Cornell and Schwertmann, 1996).

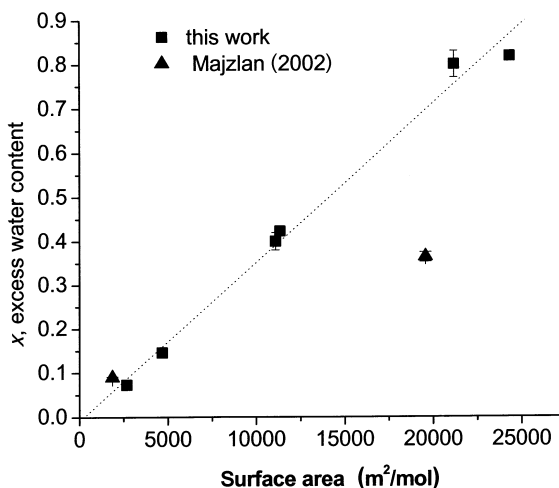


Figure 2. Correlation between the surface area of goethite and the amount of adsorbed water.

The results of oxide-melt and acid calorimetry are shown in Table 4. For each sample, the reported enthalpy of drop solution, ΔH_{ds} , or enthalpy of solution, ΔH_{sol} , represents the mean of several measurements with an associated error of two standard deviations of the mean. The thermodynamic cycles for ΔH_f^0 calculation from high-temperature and acid-solution calorimetry are given in Tables 2 and 3. As coarse-grained goethite does not dissolve rapidly enough in 5 N HCl, the expected values of ΔH_{sol} for coarse-grained goethite were calculated using ΔH_f^0 , obtained from oxide-melt calorimetry in the following way:

$$\Delta H_{sol(\alpha\text{-FeOOH})} = \Delta H_f^0(\alpha\text{-FeOOH}) - \Delta H_f^0(\gamma\text{-FeOOH}) - \Delta H_{sol(\gamma\text{-FeOOH})},$$

where $\Delta H_f^0(\alpha\text{-FeOOH})$ is the value taken from high-temperature calorimetry (Table 5), $\Delta H_{sol(\gamma\text{-FeOOH})}$ and $\Delta H_f^0(\gamma\text{-FeOOH})$ taken from Majzlan *et al.* (2003, 2004, respectively).

This calculation is reliable as these samples have low surface area and their ΔH_f^0 are in close agreement with values reported in the literature (Barany, 1965; Majzlan *et al.*, 2003). Without using data for coarse-grained samples, the acid-solution calorimetry results cannot be used to determine the surface enthalpy of goethite, as a data set with only four fine-grained samples does not cover a wide enough range of surface areas to constrain the slope of the line. A point near zero surface area is essential for accurate slope determination.

The enthalpy of formation, ΔH_f^0 , of the goethite samples from the elements (ΔH_6 , Table 2; ΔH_5 , Table 3) was calculated from the thermodynamic cycle given in Tables 2 and 3. Hematite and liquid water were used as reference phases for calculation of ΔH_f^0 from high-temperature calorimetric data. It is important to have as a reference phase a substance with known thermodynamic properties. This material must dissolve easily in the solvent. Since hematite does not dissolve in 5 N HCl at room temperature, bulk lepidocrocite (data from Majzlan *et al.*, 2003) was used as a reference phase. Because the exact siting of excess water in goethite and enthalpy of water desorption are unknown, we approximated the excess water as bulk liquid water with zero

Table 2. Thermodynamic cycle and reference calorimetric data for calculation of enthalpy of formation ΔH_f of nanophase oxides for oxide-melt calorimetry.

Reaction	Enthalpy of reaction
$\alpha\text{-FeOOH}_{\text{cr}, 25^\circ\text{C}} \cdot x\text{H}_2\text{O}_{\text{l}, 25^\circ\text{C}} = \frac{1}{2}\alpha\text{-Fe}_2\text{O}_3\text{soln, 701^\circ\text{C}} + (\frac{1}{2}+x)\text{H}_2\text{O}_{\text{g}, 701^\circ\text{C}}$	$\Delta H_1 = \Delta H_{\text{ds}(\alpha\text{-FeOOH}\cdot x\text{H}_2\text{O})}$
$\text{Fe}_{\text{cr}, 25^\circ\text{C}} + \frac{1}{2}\text{O}_{2\text{g}, 25^\circ\text{C}} = \alpha\text{-Fe}_2\text{O}_3\text{cr, 25^\circ\text{C}}$	$\Delta H_2 = \Delta H_{\text{f}^0(\alpha\text{-Fe}_2\text{O}_3\text{cr})} = -826.2 \pm 1.3 \text{ kJ/mol}^{\text{a}}$
$\text{H}_2\text{g, 25^\circ\text{C}} + \frac{1}{2}\text{O}_{2\text{g, 25^\circ\text{C}}} = \text{H}_2\text{O}_{\text{l, 25^\circ\text{C}}}$	$\Delta H_3 = \Delta H_{\text{f}^0(\text{H}_2\text{O, 25^\circ\text{C}})} = -285.8 \pm 0.1 \text{ kJ/mol}^{\text{a}}$
$\alpha\text{-Fe}_2\text{O}_3_{\text{cr, 25^\circ\text{C}}} = \alpha\text{-Fe}_2\text{O}_3\text{soln, 701^\circ\text{C}}$	$\Delta H_4 = \Delta H_{\text{ds}(\alpha\text{-Fe}_2\text{O}_3)} = 93.4 \pm 0.8^{\ddagger} (10)^{\ddagger} \text{ kJ/mol}$
$\text{H}_2\text{O}_{\text{l, 25^\circ\text{C}}} = \text{H}_2\text{O}_{\text{g, 701^\circ\text{C}}}$	$\Delta H_5 = 68.9 \text{ kJ/mol}^{\text{a}}$
$\text{Fe}_{\text{cr, 25^\circ\text{C}}} + \text{O}_{2\text{g, 25^\circ\text{C}}} + \frac{1}{2}\text{H}_2\text{g, 25^\circ\text{C}} = \alpha\text{-FeOOH}_{\text{cr, 25^\circ\text{C}}}$	$\Delta H_6 = \Delta H_{\text{f}^0(\alpha\text{-FeOOH})} = -\Delta H_1 + 0.5\Delta H_2 + 0.5\Delta H_3 + 0.5\Delta H_4 + (\frac{1}{2}+x)\Delta H_5$

^{*} average[†] two standard deviations of the mean[‡] Robie and Hemingway (1995)[‡] number of measurements

enthalpy of desorption. The low temperature of water loss in thermal analysis supports this approximation. Calculated enthalpies of formation are shown in Table 5. The relationships between enthalpy of formation and enthalpy of dissolution of goethite and surface area (in m^2/mol) are shown in Figures 3 and 4. The surface enthalpy of goethite is equal to the slope of the best-fit line obtained by least-squares regression of the data with the confidence interval of regression set at 0.90–0.98 (Zar, 1974). The enthalpy of formation of bulk goethite is equal to the intercept of the fitted line. Results (Table 5) show that the enthalpy of formation of goethite varies by 15–20 kJ/mol as a function of particle size for the range of particle sizes used in these experiments. The enthalpy changes (ΔH_{trans}) for the reaction between goethite and hematite are plotted in Figure 5.

DISCUSSION

Enthalpy of formation

Enthalpies of formation of goethite with zero surface area and nominal composition FeOOH , $-561.5 \pm 1.5 \text{ kJ/mol}$ (oxide-melt calorimetry) and $-563.9 \pm 1.6 \text{ kJ/mol}$ (acid-solution calorimetry) determined in this study are in agreement with each other within the experimental error as well as with previously reported data (Table 6). The recently obtained value of $-560.7 \pm 1.2 \text{ kJ/mol}$ (Majzlan *et al.*, 2003) is for goethite

having a surface area of $21 \text{ m}^2/\text{g}$ and the older value of $-559.4 \pm 1.3 \text{ kJ/mol}$ (Barany, 1965) is for a natural goethite with unreported surface area. The only value reported earlier for goethite with a zero surface area ($-562.9 \pm 1.5 \text{ kJ/mol}$), is that deduced by Diakonov *et al.* (1994) by reviewing Ferrier's (1966) data and agrees with our values within experimental error. But Diakonov *et al.* (1994) emphasized that their value for surface enthalpy should be considered as a rough estimate because of large uncertainties associated with surface area calculation for small grains. Additionally, due to lack of data, the surface area was estimated from synthesis conditions. Lastly, the fact that goethite with non-zero surface area always contains some adsorbed water had not been taken into account in some of the previous work.

Surface enthalpy

The values obtained for surface enthalpy, assuming adsorbed water as a bulk water and $\Delta H_{\text{des}} = 0$, are $0.60 \pm 0.10 \text{ J/m}^2$ (calculated from high-temperature oxide-melt calorimetry data) and $0.86 \pm 0.30 \text{ J/m}^2$ (calculated from acid calorimetry). Increased scatter and fewer data points can explain the larger error for the surface enthalpy obtained from acid-solution calorimetry data. Both values agree within the propagated error. We choose the value $0.60 \pm 0.10 \text{ J/m}^2$, obtained from high-temperature calorimetry, as being more accurate.

Table 3. Thermodynamic cycle and reference calorimetric data for calculation of enthalpy of formation ΔH_f of nanophase oxides for acid-solution calorimetry.

Reaction	Enthalpy of reaction
$\alpha\text{-FeOOH}_{\text{cr, 25^\circ\text{C}}} \cdot x\text{H}_2\text{O}_{\text{l, 25^\circ\text{C}}} + [3\text{H}^+]_{\text{aq, 25^\circ\text{C}}} = [\text{Fe}^{3+} + (2+x)\text{H}_2\text{O}]_{\text{aq, 25^\circ\text{C}}}$	$\Delta H_1 = \Delta H_{\text{sol}(\alpha\text{-FeOOH}\cdot x\text{H}_2\text{O})}$
$\gamma\text{-FeOOH}_{\text{cr, 25^\circ\text{C}}} \cdot w\text{H}_2\text{O}_{\text{l, 25^\circ\text{C}}} + [3\text{H}^+]_{\text{aq, 25^\circ\text{C}}} = [\text{Fe}^{3+} + (2+w)\text{H}_2\text{O}]_{\text{aq, 25^\circ\text{C}}}$	$\Delta H_2 = \Delta H_{\text{sol}(\gamma\text{-FeOOH}\cdot w\text{H}_2\text{O})} = -46.5 \pm 0.2 \text{ kJ/mol}^{\text{a}}$
$\text{H}_2\text{O}_{\text{l, 25^\circ\text{C}}} = \text{H}_2\text{O}_{\text{aq, 25^\circ\text{C}}}$	$\Delta H_3 = \Delta H_{\text{dilution}} = -0.4 \text{ kJ/mol}^{\text{a}}$
$\text{Fe}_{\text{cr, 25^\circ\text{C}}} + \text{O}_{2\text{g, 25^\circ\text{C}}} + \frac{1}{2}\text{H}_2\text{g, 25^\circ\text{C}} = \gamma\text{-FeOOH}_{\text{cr, 25^\circ\text{C}}}$	$\Delta H_4 = \Delta H_{\text{f}^0(\gamma\text{-FeOOH})} = -549.4 \pm 1.4 \text{ kJ/mol}^{\text{b}}$
$\text{Fe}_{\text{cr, 25^\circ\text{C}}} + \text{O}_{2\text{g, 25^\circ\text{C}}} + \frac{1}{2}\text{H}_2\text{g, 25^\circ\text{C}} = \alpha\text{-FeOOH}_{\text{cr, 25^\circ\text{C}}}$	$\Delta H_5 = \Delta H_{\text{f}^0(\alpha\text{-FeOOH})} = -\Delta H_1 + \Delta H_2 + (x-w)\Delta H_3 + \Delta H_4$

^a Majzlan *et al.* (2004)^b Majzlan *et al.* (2003)

Table 4. Measured ΔH_1 , and calculated ΔH^*_1 , calorimetric data of nanophase goethite.

	High-temperature calorimetry			Acid-solution calorimetry		
	ΔH_1 (kJ/g)	ΔH_1 (kJ/mol of $\alpha\text{-FeOOH}\cdot x\text{H}_2\text{O}$)	ΔH^*_1 (kJ/mol) ^a	ΔH_1 (kJ/g)	ΔH_1 (kJ/mol of $\text{FeOOH}\cdot x\text{H}_2\text{O}$)	ΔH^*_1 (kJ/mol) ^a
Bulk	1.00	90.2 \pm 0.9 [†] (10) [‡]	85.3 \pm 1.0	—	—	-35.9 \pm 1.3**
30 nm	1.02	93.7 \pm 0.2 (15)	83.6 \pm 0.3	—	—	-37.4 \pm 0.9**
9 nm	1.11	107.5 \pm 1.5 (8)	79.9 \pm 2.0	-0.41	-39.2 \pm 0.2 (3)	-39.0
7 nm	1.14	109.9 \pm 1.2 (8)	80.8 \pm 1.3	-0.43	-41.7 \pm 0.1 (4)	-41.5
5 nm	1.24	130.0 \pm 0.3 (9)	74.9 \pm 2.1	-0.48	-49.9 \pm 0.3 (4)	-49.6
2 nm	1.24	127.5 \pm 1.3 (7)	71.1 \pm 1.4	-0.52	-53.9 \pm 0.6 (4)	-53.6

* average † two standard deviations of the mean ‡ number of measurements

^a water-corrected value ΔH^*_1 kJ/mol of $\alpha\text{-FeOOH}$ was calculated as $\Delta H^*_1 = \Delta H_1 - x\cdot\Delta H_5 = \Delta H_1 - x\cdot68.9$ for high-temperature solution calorimetry and $\Delta H^*_1 = \Delta H_1 - x\cdot\Delta H_3 = \Delta H_1 + x\cdot0.4$ for acid-solution calorimetry, where x is moles of excess water

** values are recalculated using ΔH_f^0 obtained from oxide-melt calorimetry (see Table 3)

The comparison of surface enthalpy obtained in this study and previously reported data is shown in Table 6. The surface enthalpy reported by Majzlan (2002), 0.27 ± 0.12 J/m², is substantially lower and may be explained by an insufficient data set, represented by only two data points. Moreover, his fine-grained sample does not lie in the same trend as our data set (see Figures 2 and 4). Our value for the surface enthalpy of goethite is approximately half the magnitude of those obtained by Ferrier (1966) who reported the enthalpy of dissolution of different sized hematite and goethite and discussed the energetics of reaction 1. Despite calculating the enthalpy of dissolution of goethite based on two moles of FeOOH, the reported surface area is per mole of FeOOH. The surface area should be twice that given, yielding a surface energy of half the reported value, *i.e.* 0.63 J/m². This corrected value is in good agreement with our data.

High-temperature oxide-melt calorimetry for nanophase goethite

The advantage of using both acid-solution calorimetry and oxide-melt solution calorimetry on the same samples is that this combination eliminates possible concerns about high-temperature calorimetric data,

related to high water content in some samples (possible water loss during dropping the sample into the calorimeter). Moreover, the data were checked using two different thermodynamic cycles to calculate formation enthalpy, ΔH_f^0 , and surface enthalpy ΔH_s . The concordance of acid-solution and oxide-melt calorimetric data for the same samples strongly suggests that no problems were encountered with either technique.

The agreement of both techniques suggests that one can use high-temperature oxide-melt calorimetry for highly hydrated substances, in particular fine-grained goethite. There is no evidence that water loss before the sample reaches the thermopile in the hot zone of the calorimetric chamber skews data. Moreover, oxide-melt calorimetry has an advantage in comparison with acid-solution calorimetry in that even bulk and coarse-grained samples are easily dissolved in the melt and the whole particle-size range can be studied. This leads to the second advantage – the ability to use a better-investigated reference phase, hematite, rather than lepidocrocite. All these factors make the thermodynamic values (enthalpy of formation of bulk goethite = -561.5 ± 1.5 kJ/mol and surface enthalpy of goethite = 0.60 ± 0.10 J/m²) obtained by high-temperature calorimetry more reliable. Moreover, the good agreement

Table 5. Energetics of nanophase goethites in comparison to $\frac{1}{2}(\text{Fe}_2\text{O}_3 + \text{H}_2\text{O})$.

Crystallite size, nm*	Surface area (10^3 m ² /mol of FeOOH)	ΔH_f^0 (kJ/mol) acid-solution calorimetry	ΔH_f^0 (kJ/mol) oxide-melt calorimetry
2 nm	24.3	-542.3 \pm 1.5	-546.0 \pm 1.6
5 nm	21.2	-546.3 \pm 1.4	-549.7 \pm 2.3
7 nm	11.3	-554.4 \pm 1.4	-555.6 \pm 1.6
9 nm	11.1	-556.9 \pm 1.4	-554.8 \pm 2.2
30 nm	4.1	-558.5 \pm 1.7	-558.5 \pm 1.0
Bulk	2.7	-556.0 \pm 1.9	-560.1 \pm 1.4
$\frac{1}{2}(\text{Fe}_2\text{O}_3 + \text{liquid H}_2\text{O})^a$	bulk	-556.0 \pm 0.7	
$\frac{1}{2}(\text{Fe}_2\text{O}_3 + \text{gaseous H}_2\text{O})^a$	bulk		-534.0 \pm 0.1

* determined from XRD

^a from Robie *et al.* (1978)

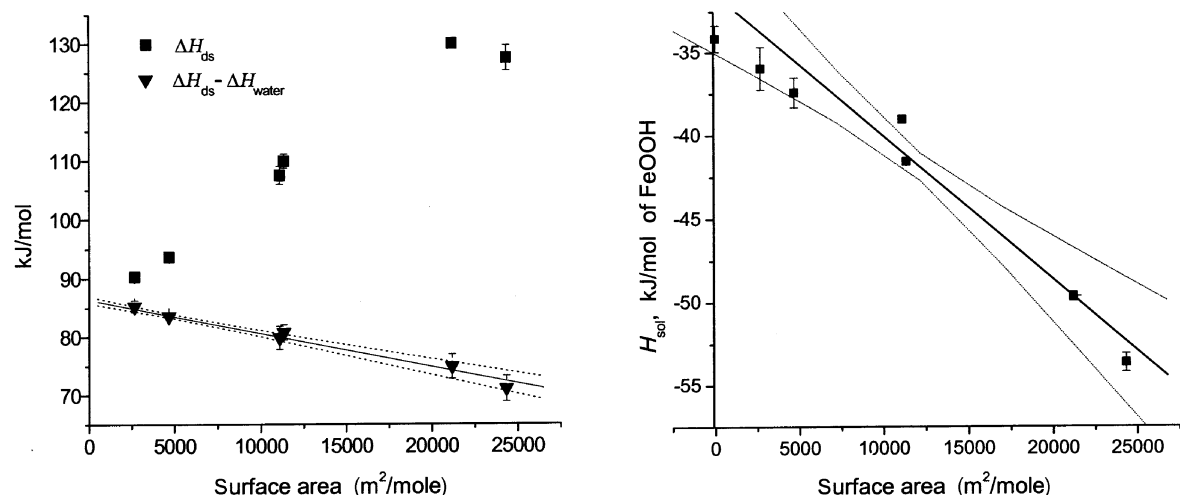


Figure 3. (a) Drop-solution enthalpy (ΔH_{ds} , kJ/mol of $\text{FeOOH}\cdot x\text{H}_2\text{O}$) and drop-solution enthalpy corrected for water ($\Delta H_{ds} - \Delta H_{\text{water}}$, kJ/mol of FeOOH); and (b) solution enthalpy (ΔH_{sol}) as a function of the surface area of goethite. The solid line is linear regression; the dashed curves represent the confidence interval of regression.

between literature heat of formation data and data obtained by high-temperature oxide-melt calorimetry (Table 6) supports the reliability of this method.

Comparison of goethite with other oxides and geological applications

A summary of surface enthalpy values for Fe and Al oxides and hydroxides is given in Table 7. Aluminum oxyhydroxide phases have lower surface enthalpy than the anhydrous phases (McHale *et al.*, 1997b; Majzlan *et al.*, 2000). One might predict a similar trend for Al and Fe oxyhydroxides. We show that goethite, a hydrated

oxide, possesses a smaller surface enthalpy compared with hematite and maghemite (see Table 7), anhydrous oxides. Having a smaller surface enthalpy allows goethite to exist with larger surface area than hematite (Figure 6). Moreover, goethite, $\alpha\text{-FeOOH}$, and lepidocrocite, $\gamma\text{-FeOOH}$, (surface enthalpies 0.60 ± 0.10 and 0.29 ± 0.13 J/ m^2 , respectively) exhibit small surface energies similar to those for boehmite (0.52 ± 0.12 J/ m^2) and gibbsite ($0.15\text{--}0.66$ J/ m^2 ; see references in Majzlan *et al.*, 2000). The estimated value by Majzlan *et al.* (2000) for diaspore, $\alpha\text{-AlOOH}$, is slightly higher than that for boehmite, but relatively close to that of goethite (see Table 7).

Another trend, observed in inorganic oxide systems, is that as metastability increases, surface enthalpy

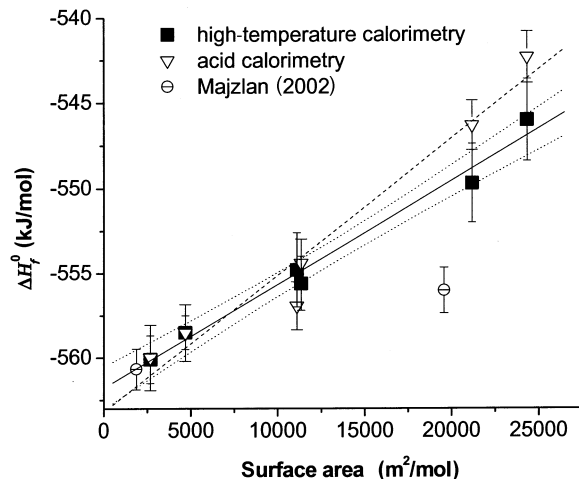


Figure 4. Calculated enthalpy of formation, (ΔH_f°), of goethite samples obtained using high-temperature calorimetry, acid-solution calorimetry at room temperature and at 70°C (data from Majzlan, 2002) as a function of surface area. The solid line and dashed line are linear regressions of high-temperature calorimetry and acid-solution calorimetry data, respectively; the dotted lines represent the 0.95 confidence interval of regression for high-temperature calorimetry data.

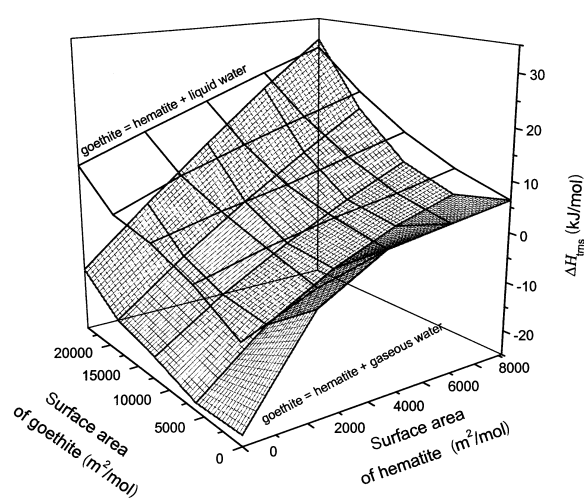


Figure 5. Enthalpy change for the reaction (ΔH_{trns}) $\text{goethite} \rightarrow \text{hematite} + \text{water}$ as a function of surface area of goethite and hematite. Surface enthalpies of hematite are taken from Majzlan (2000).

Table 6. Surface enthalpy and enthalpy of formation of bulk goethite (zero surface area).

	High-temperature calorimetry	Acid-solution calorimetry	Literature data
Surface enthalpy, ΔH_s	0.60 ± 0.10 ($R^2 = 0.99$, 0.95 confidence interval)	0.86 ± 0.30 ($R^2 = 0.87$, 0.90 confidence interval)	1.55 ± 0.20^1 $1.25 (0.63)^2$ 0.27 ± 0.12^3
ΔH_f^0 (kJ/mol, for bulk goethite)	-561.5 ± 1.5 ($R^2 = 0.99$, 0.95 confidence interval)	-563.9 ± 1.6 ($R^2 = 0.99$, 0.98 confidence interval)	-562.9 ± 1.5^1 -559.4 ± 1.3^4 -560.7 ± 1.2^5

¹ Diakonov *et al.* (1994)² Ferrier (1966) (for the value in brackets see text)⁴ Barany (1965)³ Majzlan (2002)⁵ Majzlan *et al.* (2003)

decreases (Navrotsky, 2003). Rutile, the most stable TiO_2 modification, has the largest surface enthalpy (2.2 ± 0.2 J/m²), while its metastable modifications – brookite and anatase – have surface enthalpies of 1.0 ± 0.2 J/m² and 0.4 ± 0.1 J/m², respectively (Ranade *et al.*, 2002). The surface enthalpy of monoclinic ZrO_2 is 6.5 ± 0.2 J/m², and it decreases significantly for the less stable tetragonal and amorphous ZrO_2 (surface enthalpies 2.1 ± 0.05 J/m² and 0.5 ± 0.05 J/m², respectively) (Pitcher *et al.*, 2005). Thus, similar trends hold for Al_2O_3 , $AlOOH$ and $FeOOH$ (see Table 7). However, the γ -modification of Fe_2O_3 , (maghemite) appears to have a larger surface enthalpy than the stable polymorph hematite, α - Fe_2O_3 (see Table 7). This observation requires further investigation.

Goethite and hematite are the most stable Fe oxyhydroxide and oxide phases, respectively, and have similar thermodynamic stability. Nevertheless, goethite associations with hematite in soils are found only in warm climates where dehydroxylation can occur due to

higher temperatures (Cornell and Schwertmann, 1996). Hematite alone occurs very rarely in soils. The surface enthalpy of goethite obtained in our work resolves the inconsistency between experimental energetics for the goethite-hematite equilibrium and observations for natural systems. As in the boehmite-corundum equilibrium, surface enthalpy of goethite is less (by ~20%) than that of hematite. Figure 5 shows the enthalpy of transformation of goethite to hematite and water (both liquid and gaseous) as a function of surface area. The enthalpy of dehydration becomes more positive (destabilizing the anhydrous phase) as the surface area of both phases increases to the same extent. This destabilizes the anhydrous assemblage for fine-grained materials and pushes the dehydration equilibrium to higher temperature. Figure 6 shows the relative energetics of goethite and hematite depending on surface area. The hydrous phases are thermodynamically more favored as fine materials, whereas anhydrous forms are more favored as coarse assemblages. Similar trends have been observed

Table 7. Surface enthalpies at 25°C.

Phase	Surface enthalpy (J/m ²)	Source
Oxides		
α - Al_2O_3 (corundum)	2.64 [†]	McHale <i>et al.</i> (1997a)
γ - Al_2O_3	1.66 [†]	McHale <i>et al.</i> (1997a)
α - Fe_2O_3 (hematite)	$0.77 \pm 0.2^*$	Ferrier (1966)
	1.1 ± 0.2	Diakonov <i>et al.</i> (1994)
	$0.75 \pm 0.16^*$	Majzlan (2002)
γ - Fe_2O_3 (maghemite)	$0.83 \pm 0.18^*$	Majzlan (2002)
Oxyhydroxides		
γ - $AlOOH$	$0.52 \pm 0.12^*$	Majzlan <i>et al.</i> (2000)
α - $AlOOH$ (2000)	0.2–0.8	Estimated, Majzlan <i>et al.</i>
γ - $FeOOH$	$0.29 \pm 0.13^*$	Majzlan (2002)
α - $FeOOH$	0.63	Calculated from Ferrier (1966)
	$0.27 \pm 0.12^*$	Majzlan (2002)
	$0.60 \pm 0.10^*$	This work

[†] adsorption enthalpy is taken into account^{*} calorimetric results are water corrected, but adsorbed water assumed to have bulk water energetics

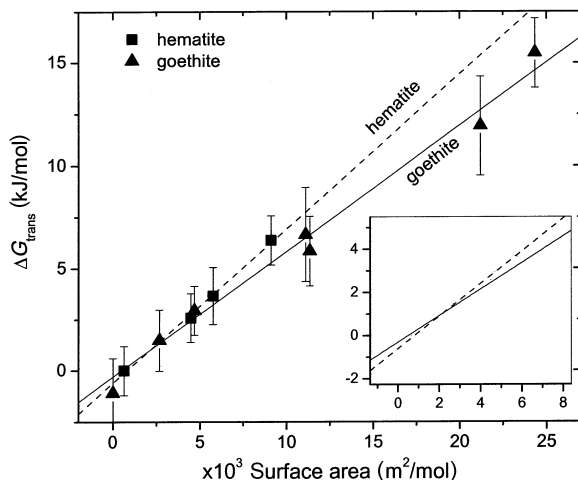


Figure 6. Gibbs free energy of transformation of goethite → hematite + liquid water and of bulk hematite → coarse hematite. The calculations were done assuming zero value of surface entropy. ΔG_f^0 of bulk hematite is taken from Robie and Hemingway (1995) (-744.4 ± 1.3 kJ/mol); ΔG_f^0 of bulk goethite was calculated using ΔH_f^0 obtained in this work (-561.5 ± 1.5 kJ/mol).

for the lepidocrocite-maghemitic (Majzlan, 2002) and for the boehmite-corundum equilibria (Majzlan *et al.*, 2000).

CONCLUSIONS

Enthalpy of formation and surface enthalpy of goethite were determined by acid-solution calorimetry and by high-temperature oxide-melt calorimetry. Data are in agreement within the experimental error. High-temperature oxide-melt calorimetry has more advantages, such as easier dissolution of coarse-grained samples and usage of better investigated reference phases and therefore the data are more reliable. Enthalpy of formation and surface enthalpy of goethite are determined by oxide-melt calorimetry to be -561.5 ± 1.5 kJ/mol and 0.60 ± 0.10 J/m², respectively. The data on enthalpy of formation are in agreement with the previously reported data. The smaller surface enthalpy of goethite, as was reported previously, resolves inconsistencies of hematite-goethite co-existence as a function of particle size.

ACKNOWLEDGMENTS

We acknowledge the National Center for Electron Microscopy at the Lawrence Berkeley National Laboratory for the use of its facilities and Dr T. Dieckmann for allowing use of the freeze dryer. We thank S. Deore for his assistance in preparing the plots, S. Ushakov for TEM analysis and M. Wang for SEM measurements. This work was supported by DOE grant DEFG0397SF14749.

REFERENCES

- Barany, R. (1965) *Heats of formation of goethite, ferrous vanadate and manganese molybdate*. US Department of the Interior, Bureau of Mines, Report of Investigation 6618.
- Brunauer, S., Emmett, P.H. and Teller, E. (1938) Adsorption of gases in multimolecular layers. *Journal of the American Chemical Society*, **60**, 309–319.
- Cohen, D.R., Shen, X.C., Dunlop, A.C. and Rutherford, N.F. (1998) A comparison of selective extraction soil geochemistry and biogeochemistry in the Cobar area, New South Wales. *Journal of Geochemical Exploration*, **61**, 367–370.
- Cornell, R.M. and Schwertmann, U. (1996) *The Iron Oxides: Structure, Properties, Reactions, Occurrence and Uses*. VCH, Germany, 573 pp.
- Crespo, M.T., del Villar, L.P., Quejido, A.J., Sánchez, M., Cázar, J.S. and Fernández-Díaz, M. (2003) U-series in Fe-U-rich fracture fillings from the oxidised cap of the ‘Mina Fe’ uranium deposit (Spain): implications for processes in a radwaste repository. *Applied Geochemistry*, **18**, 1251–1266.
- Diakonov, I., Khodakovskiy, I., Schott, J. and Sergeeva, E. (1994) Thermodynamic properties of iron oxides and hydroxides. I. Surface and bulk thermodynamic properties of goethite (α -FeOOH) up to 500 K. *European Journal of Mineralogy*, **6**, 967–983.
- Dixon, J.B. (1991) Roles of clays in soils. *Applied Clay Science*, **5**, 489–500.
- Duff, M.C., Coughlin, J.U. and Hunter, D.B. (2002) Uranium co-precipitation with iron oxide minerals. *Geochimica et Cosmochimica Acta*, **66**, 3533–3547.
- Ferrier, A. (1966) Influence de l’état de division de la goethite et de l’oxyde ferrique sur leurs chaleurs de réaction. *Revue de Chimie minérale*, **3**, 587.
- Hiemstra, T. and Van Riemsdijk, W.H. (1996) A surface structural approach to ion adsorption: the charge distribution (CD) model. *Journal of Colloid and Interface Science*, **179**, 488–508.
- Kaiser, K. (2003) Sorption of natural organic matter fractions to goethite (α -FeOOH): effect of chemical composition as revealed by liquid-state ¹³C NMR and wet-chemical analysis. *Organic Geochemistry*, **34**, 1569–1579.
- Kosmulski, M. and Maczka, E. (2004) Dilatometric study of the adsorption of heavy-metal cations on goethite. *Langmuir*, **20**, 2320–2323.
- Kosmulski, M., Saneluta, S. and Maczka, E. (2003) Electrokinetic study of specific adsorption of cations on synthetic goethite. *Colloids and Surfaces A: Physicochemical and Engineering Aspects*, **222**, 119–124.
- Langmuir, D. (1971) Particle size effect on the reaction goethite = hematite + water. *American Journal of Science*, **277**, 788–791.
- Lehmann, M., Zouboulis, A.I. and Matis, K.A. (2001) Modeling the sorption of metals from aqueous solutions on goethite fixed-beds. *Environmental Pollution*, **113**, 121–128.
- Li, P., Miser, D.E., Rabiei, S., Yadav, R.T. and Hajaligol, M.R. (2003) The removal of carbon monoxide by iron oxide nanoparticles. *Applied Catalysis B: Environmental*, **43**, 151–162.
- Lower, S.K., Tadanier, C.J. and Hochella, M.F. (2000) Measuring interfacial and adhesion forces between bacteria and mineral surfaces with biological force microscopy. *Geochimica et Cosmochimica Acta*, **64**, 3133–3139.
- Lützenkirchen, B.J., Balmès, O., Beattie, J. and Sjöberg, S. (2001) Modeling proton binding at the goethite (α -FeOOH)-water interface. *Colloids and Surfaces A: Physicochemical and Engineering Aspects*, **179**, 11–27.
- Majzlan, J. (2002) Thermodynamics of iron and aluminum oxides. PhD dissertation, University of California at Davis, Davis, CA, USA.
- Majzlan, J., Navrotsky, A. and Casey, W.H. (2000) Surface enthalpy of boehmite. *Clays and Clay Minerals*, **48**, 699–707.
- Majzlan, J., Grevel, K.D. and Navrotsky, A. (2003)

- Thermodynamics of iron oxides. II. Enthalpies of formation and relative stability of goethite (α -FeOOH), lepidocrocite (γ -FeOOH), and maghemite (γ -Fe₂O₃). *American Mineralogist*, **88**, 855–859.
- Majzlan, J., Navrotsky, A. and Schwertmann, U. (2004) Thermodynamics of iron oxides: Part III. Enthalpies of formation and stability of ferrihydrite (\sim Fe(OH)₃), schwertmannite (\sim FeO(OH)_{3/4}(SO₄)_{1/8}), and ϵ -Fe₂O₃. *Geochimica et Cosmochimica Acta*, **68**, 1049–1059.
- Manceau, A. and Charlet, L. (1994) The mechanism of selenate adsorption on goethite and hydrous ferric oxide. *Journal of Colloid and Interface Science*, **168**, 87–93.
- McHale, J.M., Aurooux, A., Perrotta, A.J. and Navrotsky, A. (1997a) Surface energetics and thermodynamic phase stability in nanocrystalline aluminas. *Science*, **277**, 788–791.
- McHale, J.M., Navrotsky, A. and Perrotta, A.J. (1997b) Effects of increased surface area and chemisorbed H₂O on the relative stability of nanocrystalline γ -Al₂O₃ and α -Al₂O₃. *Journal of Physical Chemistry*, **101**, 603–613.
- Navrotsky, A. (1997) Progress and new directions in high temperature calorimetry: revisited. *Physics and Chemistry of Minerals*, **24**, 222–241.
- Navrotsky, A. (2003) Energetics of nanoparticle oxides: interplay between surface energy and polymorphism. *Geochemical Transactions*, **4**, 34–37.
- Navrotsky, A. (2004) Environmental nanoparticles. Pp. 1147–1155 in: *Dekker Encyclopedia of Nanoscience and Nanotechnology* (J.A. Schwartz-Christian and C.-K. Putyera, editors). Marcel Dekker, New York.
- Navrotsky, A., Rapp, R.P., Smelik, E., Burnley, P., Circone, S., Chai, L. and Bose, K. (1994) The behavior of H₂O and CO₂ in high-temperature lead borate solution calorimetry of volatile-bearing phases. *American Mineralogist*, **79**, 1099–1109.
- Ottley, C.J., Davison, W. and Edmunds, W.M. (1997) Chemical catalysis of nitrate reduction by iron (II). *Geochimica et Cosmochimica Acta*, **61**, 1819–1828.
- Pitcher, M.W., Ushakov, S.V., Navrotsky, A., Woodfield, B.F., Li, G., Boero-Goates, J. and Tissie B.M. (2005) Energy crossovers in nanocrystalline zirconia. *Journal of the American Ceramic Society*, **88**, 160–167.
- Ranade, M.R., Navrotsky, A., Zhang, H.Z., Banfield, J.F., Elder, S.H., Zaban, A., Borse, P.H., Kulkarni, S.K., Doran, G.S. and Whitfield H.J. (2002) Energetics of nanocrystalline TiO₂. *Proceedings of the National Academy of Science*, **99**, 6476–6481.
- Robie, R.A. and Hemingway, B.S. (1995) Thermodynamic properties of minerals and related substances at 298.15 K and 1 bar (10⁵ pascals) and at higher temperatures. *US Geological Survey Bulletin*, **2131**, 461 pp.
- Schwertmann, U. and Cornell, R.M. (2000) *The Iron Oxides in the Laboratory: Preparation and Characterization*. VCH, New York.
- Sudakar, C., Subbanna, G.N. and Kutty, T.R.N. (2003) Effect of anions on the phase stability of γ -FeOOH nanoparticles and the magnetic properties of gamma-ferric oxide derived from lepidocrocite. *Journal of Physics and Chemistry of Solids*, **64**, 2337–2349.
- Von Gunten, H.R., Roessler, E., Lowson, R.T., Reid, P.D. and Short, S.A. (1999) Distribution of uranium- and thorium series radionuclides in mineral phases of a weathered lateritic transect of a uranium ore body. *Chemical Geology*, **160**, 225–240.
- Zar, J.H. (1974) *Biostatistical Analysis*. Prentice-Hall, Inc, Englewood Cliffs, New York.

(Received 9 July 2004; revised 25 October 2004; Ms. 933)